Published in final edited form as:
Neurosci Lett. 2007 September 13; 424(3): 185–189. doi:10.1016/j.neulet.2007.07.035.

Grooved Pegboard Test as a Biomarker of Nigrostriatal Denervation in Parkinson's disease

Nicolaas I. Bohnen, MD, PhD[1], **Hiroto Kuwabara, MD, PhD**[2], **Gregory M Constantine, PhD**[3], **Chester A. Mathis, PhD**[4], and **Robert Y. Moore, MD, PhD**[5]

1*Departments of Radiology and Neurology, University of Michigan, Ann Arbor, MI, USA*

2*Department of Radiology, Johns Hopkins University, Baltimore, MD, USA*

3*Departments of Mathematics and Statistics, University of Pittsburgh, Pittsburgh, PA, USA*

4*Department of Radiology, University of Pittsburgh, Pittsburgh, PA, USA*

5*Department of Neurology, University of Pittsburgh, Pittsburgh, PA, USA*

Abstract

Recent pharmacotherapy trials in Parkinson' disease (PD) using dopaminergic neuroimaging as outcome parameter failed to show significant relationships between imaging and clinical results. One possible explanation is that there is a non-linear relationship between striatal denervation and motor performance reflecting a statistical "floor" effect in the imaging data with advanced disease. Both the motor manifestations and the striatal dopamine denervation of idiopathic PD, however, are typically asymmetric and more meaningful associations may be found by comparing data from the least denervated striatum with motor performance in the corresponding body side. PD patients (n=28) underwent [^{11}C]β-CFT dopamine transporter (DAT) positron emission tomography (PET) and grooved pegboard testing. Voxel-based analysis of DAT PET and bimanual pegboard scores demonstrated significant correlation clusters within the bilateral striata ($P<0.001$). However, findings were most prominent in the least denervated striatum. There was a significant inverse correlation between pegboard scores of the least affected arm and DAT binding of the least denervated striatum ($Rs = -0.69$, $P<0.0001$) but no significant correlation between pegboard scores of the clinically most affected arm and DAT binding of the most denervated striatum ($Rs = -0.15$, ns). These data indicate that the robustness of the grooved pegboard test as a biomarker for nigrostriatal denervation in PD mainly reflects the relationship between test performance of the clinically least affected limb and the least denervated striatum. These findings indicate that there is both a statistical "floor" and "ceiling" effect for the most affected striatal and body sides that must be considered when employing imaging as an outcome measure in clinical trials in PD.

Keywords

Basal ganglia; [^{11}C]β-CFT; dopamine; motor functions; Parkinson's disease; pegboard; PET

Correspondence: Nicolaas I. Bohnen, MD, PhD, Departments of Radiology, Division of Nuclear Medicine, and Neurology, The University of Michigan Medical Center, B1 G505 UH, University of Michigan Medical Center, 1500 E Medical Center Drive, Ann Arbor, MI 48109-0028, USA. TEL: 734 936 5388; FAX: 734 936 8182. E-mail: E-mail: nbohnen@umich.edu.

Introduction

The most extensively described pathological abnormality in PD is loss of dopaminergic neurons in the substantia nigra pars compacta and the ventral tegmental area with degeneration of their striatal terminals leading to typical motor symptoms of PD. These are usually asymmetric in early disease but later progress into bilateral disease [10,11,15]. The greater the neuronal loss in the substantia nigra, the lower the concentration of dopamine in the striatum. Dopaminergic denervation is not distributed evenly in the striatum in PD. There is a strong caudal-to-rostral gradient with the posterior putamen being more affected than the caudate nucleus [15]. In vivo dopaminergic imaging studies have confirmed the striatal caudal-to-rostral gradient of presynaptic dopaminergic loss [8,25], and asymmetric nigrostriatal degeneration with more severe striatal dopaminergic losses contralateral to the clinically most affected body side [5].

Imaging studies have also shown that striatal dopaminergic losses are significantly correlated with the clinical stage and severity of PD [8,27]. Previous studies have shown that measures of limb bradykinesia, especially the grooved pegboard test, best reflect the nigrostriatal defect in PD [5,28]. With the appearance of therapy aiming to rescue or protect the nigrostriatal neurons in PD, presynaptic dopaminergic radiotracer imaging studies may be used as a surrogate endpoint to evaluate effects of therapy. However, recent applications of radiotracer imaging studies have shown discrepant findings between clinical outcome versus striatal imaging changes with dopaminergic therapy [26]. Although patients treated with dopamine agonist therapy had relative preservation of striatal dopaminergic binding compared to greater striatal losses in the L-DOPA treated group, the L-DOPA patients did have significantly better clinical outcome. It has been suggested that these discrepant results may represent a pharmacological effect on radioligand binding [1]. An alternative explanation may be that nigrostriatal dopaminergic denervation has limited correlation with the clinical manifestation of this disorder because of extra-striatal or non-dopaminergic degenerations in PD [18]. A third explanation is that there is a non-linear relationship between striatal denervation and motor performance reflecting a statistical 'floor' effect in the PET data with advanced disease. Both the motor manifestations and the striatal dopamine denervation of idiopathic PD are typically asymmetric. However, most studies of dopaminergic imaging and clinical outcome in PD have used bilaterally averaged imaging and clinical findings thereby possibly diluting clinically meaningful relationships. Specific assessment of the least affected hemisphere may then reveal more robust associations with clinical findings [24]. It was the goal of the present study to examine relationships between asymmetric hemispheric nigrostriatal dopaminergic denervation in PD and test performance on the grooved pegboard test in PD.

Subjects and methods

Subjects

The study involved 28 subjects with PD: 21 males and 7 females. The mean age was 59.8_10.7 years. Patients met the UK Parkinson's Disease Society Brain Bank Research Center clinical diagnostic criteria for PD [13] and were also required to have nigrostriatal denervation on DAT PET. Patients had mild to moderate severity of disease: 9 patients in stage 1, 7 patients in stages 1.5, 5 patients in stage 2, 6 patients in stage 2.5 and one patient in stage 3 of the Hoehn and Yahr classification [10]. The mean duration of disease was 3.0±3.6 years. None of the patients had dementia. The mean mini-mental status examination (MMSE) score was 29.5±0.8 [7]. The motor UPDRS was performed to determine overall parkinsonian motor impairment [6]. The mean UPDRS motor score was 15.8±8.4. The grooved pegboard test (Lafayette Instruments, Lafayette, IN) was used as a timed motor test to assess upper limb bradykinesia. Seventeen patients were taking a variable combination of amantadine, selegeline, carbidopalevodopa, or dopamine agonists (n=9). Eleven patients were drug-naïve. Subjects on dopaminergic drugs

were examined in the morning after withholding dopaminergic drugs overnight for both clinical testing and imaging. PD patients were recruited from the movement disorders clinic at the University of Pittsburgh. The study was approved by the Institutional Review Board of the University of Pittsburgh.

Dopamine transporter PET and MRI Imaging

[^{11}C]β-CFT (2-β-carbomethoxy-3β-(4-fluorophenyl) tropane) or [^{11}C]-WIN 35,428 is a specific radioligand for the dopamine transporter. [^{11}C]β-CFT was prepared using a previously described method [22,23]. 1700±1270 Ci/mmol with a range of 6,740–934 Ci/mmol. Dynamic PET scanning was performed for 90 minutes following a bolus intravenous injection of 370 MBq of [^{11}C]β-CFT. Sequential emission scans were obtained in 3D imaging mode using an ECAT HR + tomograph (CTI PET Systems, Knoxville, TN), which acquires 63 transaxial slices (axial field-of-view: 15.2 cm; slice thickness: 2.4 mm with an in-plane resolution of 4.1 mm). A thermoplastic mask was made for each subject to minimize head movement. The scanner gantry was equipped with a Neuro-insert (CTI PET Systems, Knoxville, TN) to reduce the contribution of scattered photon events [29]. PET emission data were corrected for attenuation, scatter and radioactive decay.

A volumetric spoiled gradient recall MR image was collected for each subject using a Signa 1.5 Tesla scanner (GE Medical Systems, Milwaukee, WI) with a standard head coil. The coronal SPGR sequence (TE=5, TR=25, flip angle=40 degrees, NEX=1, slice thickness=1.5 mm, image matrix=256×192, FOV=24 cm) was acquired to maximize contrast among gray matter, white matter, and CSF and provide high-resolution delineation of cortical and subcortical structures. The MR data was cropped in preparation for alignment with the PET data using AnalyzeAVW software (BIR, Mayo Foundation, Rochester, MN). Registration of the MR and dynamic PET images was performed using a modification of the automated image registration algorithm of Woods et al. [30,31]. Volumes of interest (VOIs) were drawn on the MR to include the striatum of each hemisphere and the cerebellum. Following a modification after Brück et al. [3], the ventral and dorsal striatum were defined by dividing the striatum in two halves along its vertical axis on sagittal plane. The lower three slices were used for the ventral (ventral putamen and anteroventral striatum) and the upper 4 slices for the dorsal VOI definition (caudate nucleus and putamen). The anterior and posterior dorsal putamen was identified by dividing the total putamen into two halves along its longitudinal axis on transaxial plane. All MR-drawn VOIs were transferred to the PET data for regional sampling of radioactivity using in-house developed software (UPMC Roitool).

Regional cerebral [^{11}C]β-CFT binding potential (BP) was calculated using a two-parameter multilinear reference tissue model approach (MRTM2) [14]. The cerebellum was selected as a reference region because it contains negligible levels of dopamine, providing an estimate of nonspecific binding and free tracer concentration. Ichise et al. demonstrated that MRTM2 could be applicable to slowly-dissociating radioligands [14]. The target-to-reference ratio of blood-to-brain clearance rate constants (R1) and the lumped brain-to-blood clearance rate constant (k_2') [16,17] were estimated for each striatal region while one common value was estimated for the brain-to-blood clearance rate constant of the reference region (k2R) by minimizing total residual sums of squares across all striatal regions, a modification of a method proposed by Wu and Carson [32].

Data were analyzed using Spearman rank correlation tests. Data were analyzed using the SAS program (SAS Institute Inc., Cary, NC).

Voxel-based Image Analysis

Voxel-based analysis was performed using modules of Statistical Parametric Mapping (SPM2) software [9]. BP maps were generated by the MRTM2 approach using the cerebellum time activity curve and estimate of k_2' of VOI-based analysis for each scan. Both BP maps and MRI images were flipped in the X-direction (i.e., left-right direction) for patients with predominant right body involvement before spatial normalization. Spatial normalization was performed as following: each BP map was spatially aligned to the subject's MRI using the coregistration module of SPM2. Then each MRI was spatially normalized to a standard MRI in the orientation of the SPM T1 template using initial linear alignments followed by nonlinear warping using the spatial normalization module of SPM2. Finally, each BP map was spatially normalized in one step by combining the parameters of the coregistration and spatial normalization. Spatially normalized BP maps were smoothed using 10 mm Gaussian kernels in X, Y, and Z direction. Correlation analysis with the bimanual pegboard test score was performed using the simple regression module of SPM. Clusters with positive correlation at a $P<0.001$, uncorrected level with a minimal volume of 20 voxels were considered significant.

Results

Table 1 lists striatal and regional striatal DAT BP values contralateral and ipsilateral to the clinically most affected body side. Results demonstrate the caudal-to-rostral denervation gradient and striatal asymmetry. Striatal binding was asymmetric in all regions but most pronounced in the dorsal caudal putamen (asymmetry ratio = 0.63; $P<0.0001$; Table 1). The average pegboard scores for the clinically most and least affected arms were 129.0±42.9 and 107.4±42.9 seconds, respectively (asymmetry ratio = 0.83; $P<0.01$).

Voxel-based intrastriatal analysis of DAT PET and bimanual pegboard scores demonstrated significant correlation clusters within the bilateral striatum involving both the putamen and caudate nucleus. However, findings were most prominent in the least denervated striatum, especially the mid to ventral caudal putamen ($P<0.001$; Figure 1).

Figure 2 displays the individual scatter data plots of the associations between most versus least affected arm and denervated striatum in PD. There was no significant correlation between pegboard scores of the most affected arm (MAA) and DAT binding of the most denervated striatum ($Rs=-0.15$, ns). In contrast, there was a significant inverse correlation between pegboard scores of the least affected arm (LAA) and DAT binding of the least denervated striatum ($Rs=-0.69$, $P<0.0001$). The correlation between the pegboard score of the MAA and the least denervated striatum failed to achieve significance ($Rs=-0.35$, $P=0.06$). There was a significant correlation between pegboard test performance of the LAA and the most denervated striatum ($Rs=-0.48$, $P=0.009$).

A post hoc analysis was performed to evaluate the effect of hand dominance in relationship with predominant PD body involvement. There were 19 patients with predominant left-sided body involvement (15 were right and 4 left hand dominant). There were 9 patients with predominant right body involvement (8 were right hand and 1 left hand dominant). Analysis limited to right hand dominant patients with left body involvement (n=15) demonstrated a significant inverse correlation between LAA pegboard scores and least denervated striatum ($Rs=-0.73$, $P=0.0004$) but no significant correlation between MAA pegboard scores and most denervated striatum ($R=-0.16$, ns). Analysis limited to the right hand dominant patients with predominant left body involvement demonstrated similar correlation coefficients: $Rs=-0.68$ ($P=0.04$) and $Rs=-0.08$ (ns), respectively.

Discussion

We did not find a significant correlation between pegboard scores of the MAA and DAT binding of the most denervated striatum. In contrast, there was a significant inverse correlation between pegboard scores of the LAA and DAT binding of the least denervated striatum. Our findings indicate a statistical "floor" effect due to more severe denervation of the striatum, especially the dorsal putamen, corresponding to the clinically most affected limb. Furthermore, we found evidence for a statistical "ceiling" effect related to worsening pegboard test performance of the MAA because of better correlations between pegboard score for the LAA and the most denervated basal ganglion. Our data show a striking significant inverse correlation between pegboard test performance of the clinically LAA and DAT binding in the contralateral striatum. This is not a function of handedness as similar results were obtained when the analysis was restricted to right hand dominant subjects. These findings indicate that the wider ranges of dopaminergic innervation of the least denervated striatum and scores of the LAA pegboard provide for better quantitative assessment of clinical and imaging measures of function in PD.

The establishment of a clinical test as a relevant biomarker for nigrostriatal denervation in PD, requires that there be a proportionate relationship between the degree of striatal dopaminergic denervation and clinical impairment as shown by the test [26]. With respect to the grooved pegboard test, a measure largely of bradykinesia, our data indicate that such proportionate relationship can be shown for the extent of denervation of the least denervated compared to the most denervated striatum. Previous PET studies have reported that despite the prominent loss of dopaminergic innervation in the dorsal and caudal putamen in PD, the extent of dopaminergic loss with progression of disease is similar in different striatal regions [3,20]. Our data also show that the asymmetric nigrostriatal denervation affects all striatal regions, including the ventral striatum. The instrastriatal collinearity of dopaminergic denervation in PD may explain why the least denervated basal ganglion would provide a more robust imaging substrate for clinical biomarker definition.

Although our voxel-based instrastriatal analysis demonstrated strong putaminal clusters there were also smaller but significant clusters of voxels within the caudate nucleus, especially the least denervated side. It is believed that dopaminergic nigrostriatal connections to the caudate nucleus are more strongly related to cognition and less strongly to motility compared with those of the putamen [2]. The involvement of the caudate nucleus may reflect functions of visuospatial attention and sensorimotor integration required for optimal performance on the grooved pegboard test. An alternative explanation is that it also relates to the phenomenon of intrastriatal collinearity within the degenerating striatum in PD [20].

The present study did not include subjects with prodromal PD and it is possible that in such subjects the correlation between pegboard test performance of the MAA and striatal DAT binding would be high. There are different methodological requirements for biomarkers to be used for diagnosis versus assessment of progression of disease or outcome [4]. Whereas our findings indicate potential usefulness of the grooved pegboard test of the LAA as a progression biomarker, the use of the grooved pegboard test of the LAA as a diagnostic biomarker would limit its sensitivity.

It should also be noted that the range of nigrostriatal denervation in PD may depend on the type of dopaminergic radiotracer. DAT radiotracers will be more prone to denervation "floor" effects because of downregulation, whereas [^{18}F]fluorodopa which may show opposite findings because of increased DOPA decarboxylase and, hence, increased [^{18}F]fluorodopa storage in PD [19,28].

A possible strategy to apply biomarkers in clinical trials in the presence of statistical ‘floor’ or ‘ceiling’ effects includes the selection of subjects with (very) early disease and thereby

minimizing both statistical effects. Alternatively, a separate post hoc analysis can be performed for the most or least affected limb when studying subjects with more advanced PD. These strategies are particularly indicated for PET or SPECT analysis using traditional volume of interest technique. Recent advances in image analysis, such as spatial pattern or network analysis of functional brain images using partial least squares [21] or metabolic covariance [12], not only offer insights in regional functional connectivity but also provide measures of correlation between regional brain activity and specific clinical functions. For example, Huang *et al*. report on changes in motor and cognitive brain network activity with the progression of PD using longitudinal clinical assessment and glucose metabolic and DAT PET imaging [12]. These clinically-defined brain image pattern scores may serve as novel and integrated clinico-PET biomarkers in future outcome research in PD. These measures are also based on multivariate statistical methods that are more suited to capture non-linear relationships between imaging and clinical functions.

In conclusion, the grooved pegboard test is a robust biomarker for dopaminergic nigrostriatal denervation as shown by DAT PET in showing the relationship between test performance of the clinically least affected limb and the least denervated striatum in clinically symptomatic patients with PD. The findings indicate a double statistical "floor" and "ceiling" effect for the most denervated basal ganglion side and clinically most affected limb. This limitation needs to be considered when conducting clinical trials in which imaging is to be used as a measure of clinical outcome in PD.

Acknowledgements

The authors thank the PET technologists, cyclotron operators, chemists, Kurt Schimmel, Larry Ivanco, and study coordinators for their assistance. Supported by NIH P01 NS019608.

References

1. Albin RL, Nichols TE, Frey KA. Brain imaging to assess the effects of dopamine agonists on progression of Parkinson disease. JAMA 2002;288:311–312. [PubMed: 12117386]
2. Alexander GE, DeLong MR, Strick PL. Parallel organization of functionally segregated circuits linking basal ganglia and cortex. Annu Rev Neurosci 1986;9:357–381. [PubMed: 3085570]
3. Bruck A, Aalto S, Nurmi E, Vahlberg T, Bergman J, Rinne JO. Striatal subregional 6-[18F]fluoro-L-dopa uptake in early Parkinson's disease: a two-year follow-up study. Mov Disord 2006;21:958–963. [PubMed: 16550545]
4. Dorsey ER, Holloway RG, Ravina BM. Biomarkers in Parkinson's disease. Expert Rev Neurother 2006;6:823–831. [PubMed: 16784406]
5. Eidelberg D, Moeller JR, Dhawan V, Sidtis JJ, Ginos JZ, Strother SC, Cedarbaum J, Greene P, Fahn S, Rottenberg DA. The metabolic anatomy of Parkinson’s disease: complementary [^{18}F] fluorodeoxyglucose and [^{18}F]fluorodopa positron emission tomographic studies. Mov Dis 1990;5:203–213.
6. Fahn, S.; Elton, R. Members of the UPDRS development committee. Unified Parkinson’s disease rating scale. In: Fahn, S.; Marsden, C.; Calne, D.; Goldstein, M., editors. Recent developments in Parkinson’s disease. Florham Park, NJ: Macmillan Healthcare Information; 1987. p. 153-164.
7. Folstein MF, Folstein SE, McHugh PR. Mini-mental state: a practical method for grading the cognitive state of patients for the clinician. J Psychiatry Res 1975;12:189–198.
8. Frey KA, Koeppe RA, Kilbourn MR, Vander Borght TM, Albin RL, Gilman S, Kuhl DE. Presynaptic monoaminergic vesicles in Parkinson’s disease and normal aging. Ann Neurol 1996;40:873–884. [PubMed: 9007092]
9. Friston K, Holmes A, Worsley K, Poline J-B, Frith C, Frackowiak R. Statistical parametric maps in functional imaging: A general linear approach. Hum Brain Mapp 1995;2:189–210.
10. Hoehn M, Yahr M. Parkinsonism: onset, progression, and mortality. Neurology 1967;17:427–442. [PubMed: 6067254]

11. Hornykiewicz O. Dopamine (3-hydroxytyramine) and brain function. Pharmacol Rev 1966;18:925–965. [PubMed: 5328389]
12. Huang C, Tang C, Feigin A, Lesser M, Ma Y, Pourfar M, Dhawan V, Eidelberg D. Changes in network activity with the progression of Parkinson's disease. Brain 2007;130:1834–1846. [PubMed: 17470495]
13. Hughes AJ, Daniel SE, Kilford L, Lees AJ. Accuracy of clinical diagnosis of idiopathic Parkinson's disease: a clinicopathologic study of 100 cases. J Neurol Neurosurg Psychiatry 1992;55:181–184. [PubMed: 1564476]
14. Ichise M, Liow JS, Lu JQ, Takano A, Model K, Toyama H, Suhara T, Suzuki K, Innis RB, Carson RE. Linearized reference tissue parametric imaging methods: application to [^{11}C]DASB positron emission tomography studies of the serotonin transporter in human brain. J Cereb Blood Flow Metab 2003;23:1096–1112. [PubMed: 12973026]
15. Kish SJ, Shannak K, Hornykiewicz O. Uneven pattern of dopamine loss in the striatum of patients with idiopathic Parkinson's disease. New Eng J Med 1988;318:876–880. [PubMed: 3352672]
16. Koeppe RA, Holthoff VA, Frey KA, Kilbourn MR, Kuhl DE. Compartmental analysis of [^{11}C] flumazenil kinetics for the estimation of ligand transport rate and receptor distribution using positron emission tomography. J Cereb Blood Flow Metab 1991;11:735–744. [PubMed: 1651944]
17. Lammertsma AA, Hume SP. Simplified reference tissue model for PET receptor studies. Neuroimage 1996;4:153–158. [PubMed: 9345505]
18. Langston JW. The Parkinson's complex: parkinsonism is just the tip of the iceberg. Ann Neurol 2006;59:591–596. [PubMed: 16566021]
19. Lee CS, Samii A, Sossi V, Ruth TJ, Schulzer M, Holden JE, Wudel J, Pal PK, de la Fuente-Fernandez R, Calne DB, Stoessl AJ. In vivo positron emission tomographic evidence for compensatory changes in presynaptic dopaminergic nerve terminals in Parkinson's disease. Ann Neurol 2000;47:493–503. [PubMed: 10762161]
20. Lee CS, Schulzer M, de la Fuente-Fernandez R, Mak E, Kuramoto L, Sossi V, Ruth TJ, Calne DB, Stoessl AJ. Lack of regional selectivity during the progression of Parkinson disease: implications for pathogenesis. Arch Neurol 2004;61:1920–1925. [PubMed: 15596613]
21. McIntosh AR, Lobaugh NJ. Partial least squares analysis of neuroimaging data: applications and advances. Neuroimage 2004;23:S250–S263. [PubMed: 15501095]
22. Nagren K, Halldin C, Muller L, Swahn CG, Lehikoinen P. Comparison of [^{11}C]methyl triflate and [^{11}C]methyl iodide in the synthesis of PET radioligands such as [^{11}C]beta-CIT and [^{11}C]beta-CFT. Nucl Med Biol 1995;22:965–979. [PubMed: 8998473]
23. Nagren K, Muller L, Halldin C, Swahn CG, Lehikoinen P. Improved synthesis of some commonly used PET radioligands by the use of [^{11}C]methyl triflate. Nucl Med Biol 1995;22:235–239. [PubMed: 7767319]
24. Pirker W. Correlation of dopamine transporter imaging with parkinsonian motor handicap: How close is it? Mov Disord 2003;18:S43–S51. [PubMed: 14531046]
25. Rakshi JS, Uema T, Ito K, Bailey DL, Morrish PK, Ashburner J, Dagher A, Jenkins IH, Friston KJ, Brooks DJ. Frontal, midbrain and striatal dopaminergic function in early and advanced Parkinson's disease A 3D [^{18}F]dopa-PET study. Brain 1999;122:1637–1650. [PubMed: 10468504]
26. Ravina B, Eidelberg D, Ahlskog JE, Albin RL, Brooks DJ, Carbon M, Dhawan V, Feigin A, Fahn S, Guttman M, Gwinn-Hardy K, McFarland H, Innis R, Katz RG, Kieburtz K, Kish SJ, Lange N, Langston JW, Marek K, Morin L, Moy C, Murphy D, Oertel WH, Oliver G, Palesch Y, Powers W, Seibyl J, Sethi KD, Shults CW, Sheehy P, Stoessl AJ, Holloway R. The role of radiotracer imaging in Parkinson disease. Neurology 2005;64:208–215. [PubMed: 15668415]
27. Seibyl JP, Marek KL, Quinlan D, Sheff K, Zoghbi S, Zea-Ponce Y, Baldwin RM, Fussell B, Smith EO, Charney DS, Hoffer PB, Innis RB. Decreased single-photon emission computed tomographic [^{123}Ib-CIT striatal uptake correlates with symptom severity in Parkinson's disease. Ann Neurol 1995;38:589–598. [PubMed: 7574455]
28. Vingerhoets FJG, Schulzer M, Calne DB, Snow BJ. Which clinical sign of Parkinson's disease best reflects the nigrostriatal lesion? Ann Neurol 1997;41:58–64. [PubMed: 9005866]
29. Weinhard, K. Applications of 3D PET. In: Bendriem, B.; Townsend, DW., editors. The theory and practice of 3D PET. Boston: Kluwer Academic Publishers; 1998. p. 133-167.

30. Wiseman MB, Nichols TE, Woods RP, Sweeney JA, Mintun MA. Stereotaxic techniques comparing foci intensity and location of activation areas in the brain as obtained using positron emission tomography (PET). J Nucl Med 1995;36(suppl)

31. Woods RP, Mazziota JC, Cherry SR. MRI-PET registration with automated algorithm. J Comput Assist Tomogr 1993;17:536–546. [PubMed: 8331222]

32. Wu Y, Carson RE. Noise reduction in the simplified reference tissue model for neuroreceptor functional imaging. J Cereb Blood Flow Metab 2002;22:1440–1452. [PubMed: 12468889]

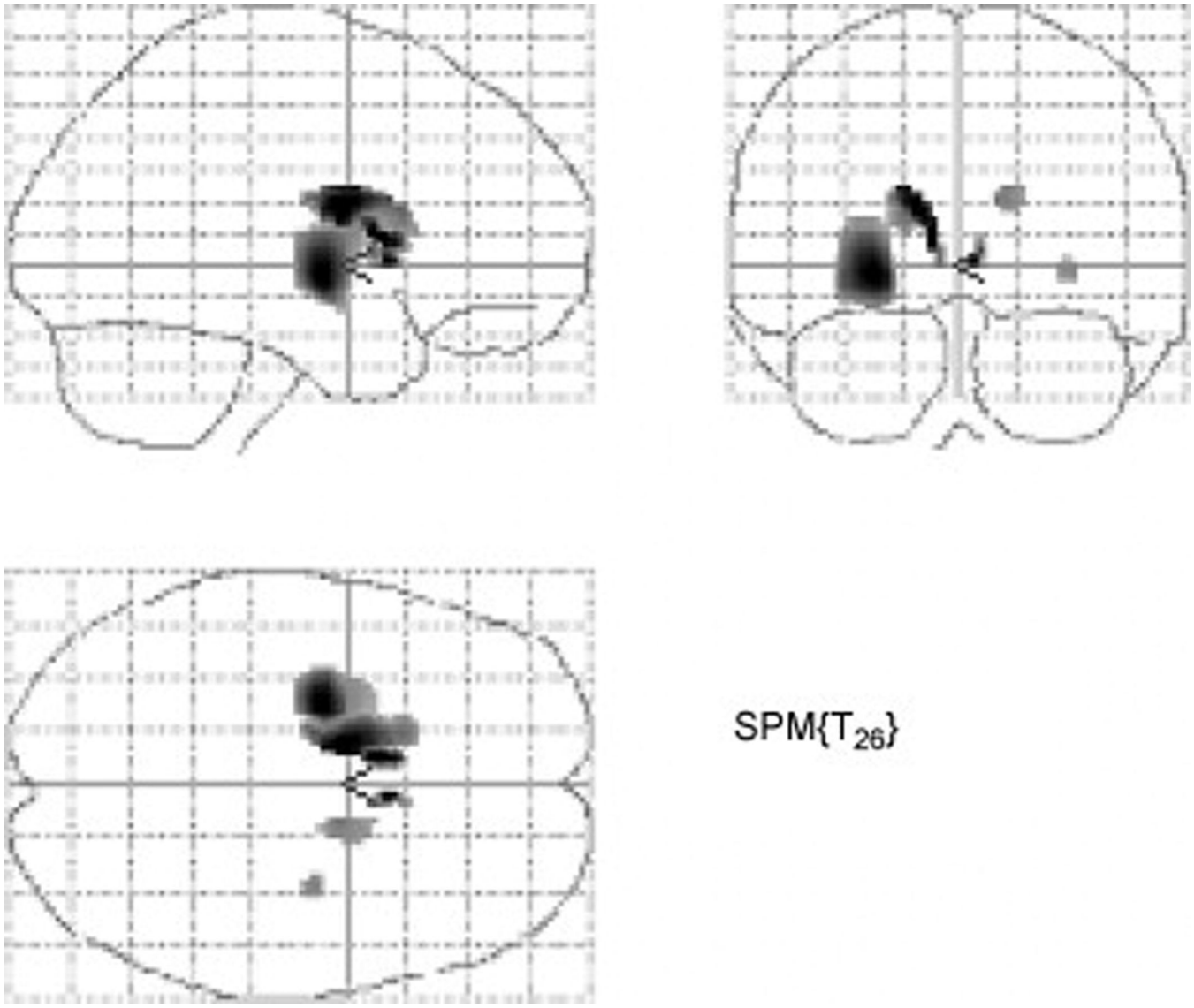

Fig. 1.

Voxel-based intrastriatal analysis of the correlation between DAT PET and bimanual pegboard scores demonstrated significant voxel clusters (P<0.001) within the striatum that were most prominent in the putamen and caudate nucleus contralateral to the clinically least affected arm. The most significant clusters are located within the mid- to ventral putamen of the least denervated hemisphere.

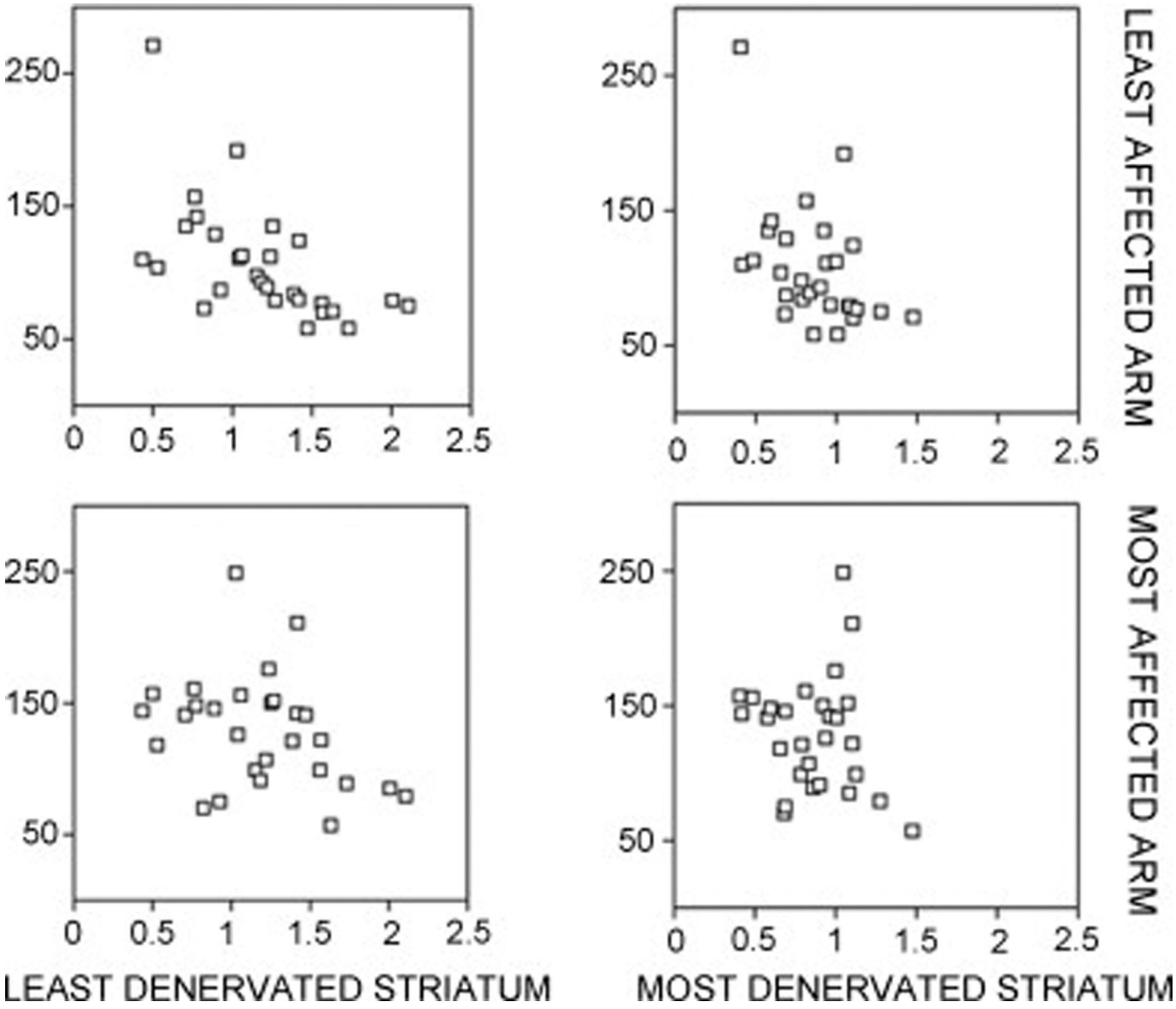

Fig. 2.
Individual scatter data plots of the associations between most versus least affected arm and denervated striatum in PD.

Table 1

Striatal and regional striatal [^{11}C]β-CFT binding potential contralateral and ipsilateral to the most affected body side for the patients are shown in Table 1. Mean (±SD) values are given.

	Striatum contralateral to clinical most affected body side	Striatum ipsilateral to clinical most affected body side	Asymmetry ratio
Total striatum	0.87±0.26	1.18±0.43	0.74 (t=6.2; P<0.0001)
Dorsal caudate nucleus	1.20±0.45	1.43±0.62	0.84 (t=4.3; P=0.0002)
Anteroventral striatum	1.1±0.33	1.34±0.46	0.82 (t=6.2; P<0.0001)
Dorsal anterior putamen	0.94±0.43	1.33±0.58	0.71 (t=5.8; P<0.0001)
Dorsal posterior putamen	0.55±0.20	0.93±0.42	0.59 (t=6.5; P<0.0001)
Ventral putamen	0.55±0.14	0.88±0.35	0.63 (t=5.6; P<0.0001)